

The symbiotic star CH Cygni. III. A precessing radio jet

M. M. Crocker¹, R. J. Davis¹, R. E. Spencer¹, S. P. S. Eyres², M. F. Bode³, A. Skopal^{3,4}

¹Jodrell Bank Observatory, University of Manchester, Macclesfield, Cheshire, SK11 9DL, UK.

²Centre for Astrophysics, University of Central Lancashire, Preston, PR1 2HE, UK

³Astrophysics Research Institute, Liverpool John Moores University, Twelve Quays House, Egerton Wharf, Birkenhead, CH41 1LD, UK

⁴Astronomical Institute, Slovak Academy of Sciences, 059 60 Tatranská Lomnica, Slovakia

Accepted ?????. Received ????; in original form ?????

ABSTRACT

VLA, MERLIN and Hubble Space Telescope imaging observations of the extended regions of the symbiotic system CH Cygni are analysed. These extensions are evidence of a strong collimation mechanism, probably an accretion disk surrounding the hot component of the system. Over 16 years (between 1985 and 2001) the general trend is that these jets are seen to precess. Fitting a simple ballistic model of matter ejection to the geometry of the extended regions suggests a period of 6520 ± 150 days, with a precession cone opening angle of 35 ± 1 degrees. This period is of the same order as that proposed for the orbital period of the outer giant in the system, suggesting a possible link between the two. Anomalous knots in the emission, not explained by the simple model, are believed to be the result of older, slower moving ejecta, or possibly jet material that has become disrupted through sideways interaction with the surrounding medium.

Key words: binaries: symbiotic – circumstellar matter – stars: imaging – stars: individual: CH Cygni – stars: late-type – radio continuum : stars

1 INTRODUCTION

Symbiotic stars occupy an extreme and relatively poorly understood region of the binary classification scheme. The name was coined by Merrill (1941) to describe stars which appeared to have a combination spectrum: that of high excitation lines usually associated with a hot, ionised nebula superimposed on a cool continuum with prominent absorption features consistent with a late-type star. At present they are understood to be interacting binaries (with orbital periods of a few to tens of years) consisting of a cool giant losing material mostly via the stellar wind and a hot, luminous compact object which ionises a portion of the cool component wind (Seaquist et al. 1984). Such a state of affairs represents the so-called *quiescent phase*, which can be interrupted by periods of activity. The *active phases* start with an eruption of the hot star, an event indicated photometrically by an increase of the star’s brightness by 2–6 mag, and/or spectroscopically by high velocity broad emission features from the central star. Both radio and Hubble Space Telescope (HST) imaging can directly resolve the remnants of such dramatic events (Hack & Paresce 1993; Eyres et al. 1995; Kenny et al. 1996; Richards et al. 1999; Eyres et al. 2001b).

The symbiotic star CH Cygni displays particularly complex behaviour. Optical spectroscopic studies by Mikolajewski et al. (1987) showed that the orbits of the stars within the

system are likely to be coplanar and eclipsing, with eclipses separated by around 5700 days. Later studies (Mikolajewski et al. 1990b and references therein) confirmed this period.

Further spectral studies of the system (Hinkle et al. 1993) suggested that CH Cyg is probably a triple-star system consisting of an inner 756-day period binary which is orbited by an unseen G-K dwarf on a 5300 day orbit. Skopal et al. (1996) uncovered 756 day interval eclipses which show that all three stars in the system are likely to be in coplanar orbits.

Each of the three outbursts seen since 1978 was accompanied by high velocity broad emission features consistent with mass outflows. During 1984–85 the material was ejected at $\sim 600\text{--}2500 \text{ km s}^{-1}$ (Mikolajewski & Tomov 1986), whilst the 1992–95 active phase was characterized by sporadic and in part bipolar outflow at $\sim 1000\text{--}1600 \text{ km s}^{-1}$ (Leedj arv & Mikolajewski 1996; Skopal et al. 1996; Iijima 1996) and finally, during the recent, 1998–2000, outburst mass outflows at about 1000 km s^{-1} were observed (Eyres et al. 2001a, hereafter Paper II). The outflows may be correlated with a significant increase of the radio emission and the radio light curves during these periods fit well with the optical ones (Kenny et al. 1996). The 1984 mass ejection has been linked to the emergence of bipolar emission (Taylor et al. 1986) which has been attributed to high velocity ($\sim 1000 \text{ km s}^{-1}$) jets. Non-thermal emission features have been discovered in

arXiv:astro-ph/0209097v1 5 Sep 2002

these jets from radio observations (Crocker et al. 2001, hereafter Paper I), explained by shocked regions that arise when the high-speed ejecta interact with existing wind material.

This paper aims to extend our understanding of the jets in this interesting system by developing theories and models to explain the change in their morphology in the years following their emergence.

In this paper we present analysis of radio data from the VLA and MERLIN, along with HST observations.

2 OBSERVATIONS

CH Cygni has been observed on several occasions since 1985, in several different radio wavelengths and optical domains, further details of which are given in Paper I. All observations have been presented previously with the exception of the 2000 November 10⁷ VLA data which is shown here for the first time.

Radio data reduction was carried out using the AIPS software package (Greisen 1999). The flux density of the phase reference source was determined, and the data calibrated to correct phase and amplitude instabilities. These corrections were applied to the observations of CH Cygni and a map produced by deconvolving the instrumental response (the so-called “dirty beam”) from the map using the well-established CLEAN algorithm (Högbom 1974).

Observations made on 1999 August 12 with the Hubble Space Telescope’s Wide Field and Planetary Camera 2 through the F502N filter, corresponding to the [O III] line at $\lambda\lambda 4956$ and 5007\AA (Biretta et al. 2001), are used here as these, with a diffraction limited resolution of around 0.05 arcseconds, offer direct comparison with the spatial resolution of the radio data (see Table 1. Each observation was made up of two sub-exposures, allowing cosmic ray subtraction to be carried out (see Paper II and references therein).

3 INITIAL DATA ANALYSIS

A preliminary examination of radio maps of CH Cygni (taken with the VLA and MERLIN), as well as the HST optical images (using the F502N [OIII] filter) show that the position angle of the extended regions changes drastically over the 15 years between the earliest (1985) and most recent (2000) observations.

A more quantitative analysis requires a measurement of the position angle of the central regions of the radio nebula. A problem inherent in this method is that the geometry of the restoring beam (in the case of the radio observations) may dominate over any natural geometry of the region. This arises as a result of the (u, v) coverage of the instrument, which depends upon the altitude of the source above the horizon.

To avoid these problems, the radio maps were recreated using the methods of Högbom (1974) but a circular restoring beam was imposed upon them, as laid out in Table 1.

Two dimensional Gaussians were fitted to the bright peak in the centre of each map, and the position angle (anticlockwise through east from north) of the semi-major axis of the resulting ellipse was taken as the position angle of the central material. The uncertainties are those produced by

Table 1. Restoring beams used at different radio observing frequencies.

Instrument	Frequency (GHz)	Beamsize (arcseconds)
VLA	1.5	1.5
	4.8	0.5
	8.4	0.25
	15.0	0.15
MERLIN	1.5	0.15
	4.9	0.05

Table 2. Position angle of the central region of the nebula of CH Cygni

Instrument	Julian Date	Year	ν (Ghz)	Position angle ($^{\circ}$)
VLA	2446087	1985	14	137.7 ± 0.3
VLA	2446509	1986	1.6	135.4 ± 1.2
VLA	2446509		4.8	133.9 ± 0.3
VLA	2446509		14	123.2 ± 1.6
VLA	2446509		22	131.1 ± 10.7
VLA	2446576		1.6	136.7 ± 1.0
VLA	2446576		4.8	132.2 ± 0.4
VLA	2446576		14	117.2 ± 0.7
VLA	2446576		22	113.3 ± 4.4
VLA	2447003	1987	1.5	134.9 ± 2.0
VLA	2447003		4.8	110.5 ± 0.5
VLA	2447003		15	91.8 ± 1.2
VLA	2447450	1988	1.6	138.9 ± 5.6
VLA	2447450		4.8	109.8 ± 4.5
VLA	2447505		14	111.7 ± 20.6
VLA	2448488	1991	4.8	112.0 ± 9.7
MERLIN	2448827	1992	4.8	121.0 ± 9.9
MERLIN	2449911	1995	4.8	125.5 ± 5.0
VLA	2449916		1.6	138.9 ± 4.8
VLA	2449916		8.4	132.0 ± 2.0
VLA	2449916		14	138.0 ± 16.8
VLA	2449949		1.6	139.5 ± 3.1
VLA	2449949		4.8	134.9 ± 1.4
VLA	2449949		8.4	126.7 ± 1.1
MERLIN	2451235	1999	4.8	174.3 ± 4.7
MERLIN	2451307		1.7	166.5 ± 7.2
HST	2451402		[OIII]	162.2 ± 0.1
VLA	2451447		4.8	164.1 ± 0.7
VLA	2451447		8.4	169.9 ± 0.8
MERLIN	2451481		1.6	166.5 ± 7.2
MERLIN	2451607	2000	4.8	200.5 ± 5.2
MERLIN	2451696		4.8	185.4 ± 8.0
VLA	2451858		1.6	177.2 ± 5.2
VLA	2451858		4.8	171.5 ± 1.4
VLA	2451858		8.4	192.2 ± 1.0
VLA	2451858		14	197.6 ± 10.3
MERLIN	2451961		4.8	198.6 ± 18.7

the AIPS task ‘IMFIT’, and are derived from the ratio of the axes of the fitted ellipse. These measurements are shown in Table 2.

Since the details of the alignment of the CH Cygni system are not known, it was assumed that the orbital plane of the system is being viewed edge-on, as eclipses are seen within the system (Mikolajewski et al. 1987; Skopal et al. 1996). The extension might be expected to precess about an axis perpendicular to the orbital plane if this is associated

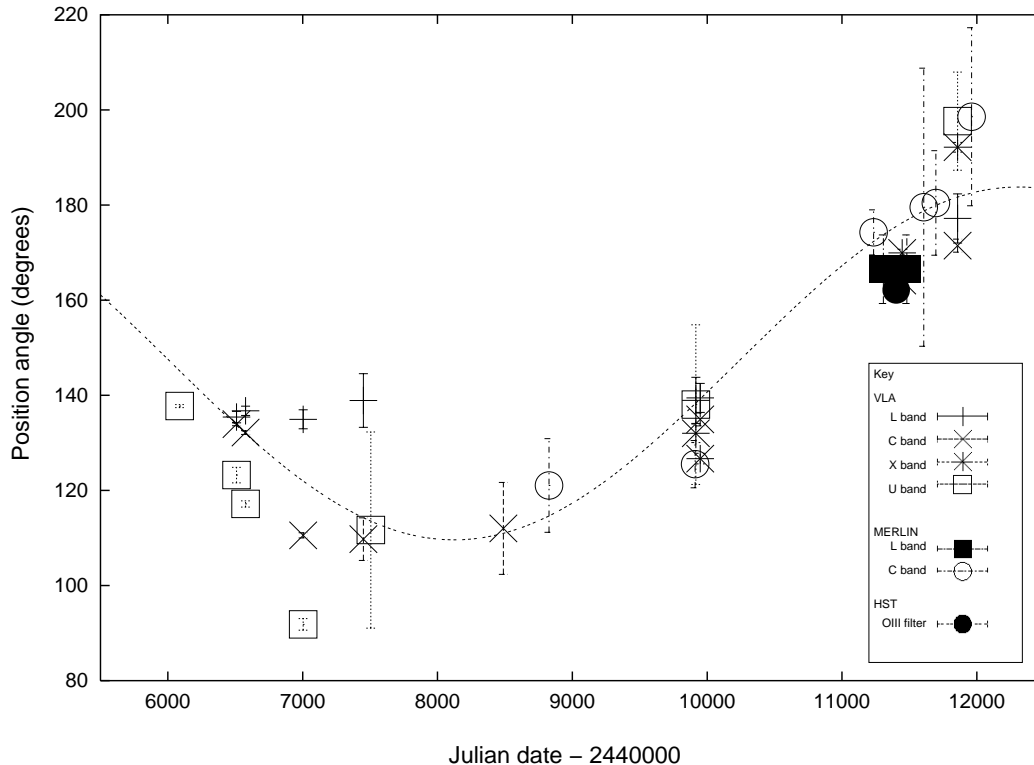


Figure 1. Variation of the position angle of the central region of CH Cygni between 1985 and 2000, along with the fitted curve described in Section 3. The fitted curve should be treated with caution as the data set does not appear to cover a full period of precession.

with the collimating mechanism. Assuming that the rate of precession is constant, the position angle, θ_{PA} should follow a simple sinusoid so that at time t the position angle is given by

$$\theta_{\text{PA}} = \theta_{\text{mid}} + \theta_{\text{o}} \cos\left(2\pi \times \frac{t - t_0}{P}\right). \quad (1)$$

Such a curve was fitted, giving a precession of period $P = 8373 \pm 800$ days about a position angle on the sky of $\theta_{\text{mid}} = 146.7 \pm 3.4$ degrees. The opening angle of the precession cone was $\theta_{\text{o}} = 37.1 \pm 4.7^\circ$.

This precession period is longer than the 5294 ± 117 day period quoted for the length of the orbit of the outer giant of the system by Hinkle et al. (1993). The precession period we see could be a resonance of this, the 756 day orbital period, or both. However, the period we find should be treated with some caution, as our data set does not appear to cover a full period of precession.

4 EVIDENCE OF PRECESSION WITHIN THE RADIO JETS

There is a large deviation of some of the points from the fitted curve. A flaw inherent in the method of fitting gaussians is that it will naturally pick up the position angle of material at a certain distance from the core – that distance being determined by the resolution of the map. Hence what is being picked up is the position angle of material that was ejected some time before the observation was made.

If the material in the extension is being ejected ballistically from a precessing source then it would be expected to trace out a conical helix of a form seen in many precessing objects (Zaninetti & van Horn 1988). Expansion has been detected in the jet since the first radio jets were seen by Taylor et al. (1986).

Precessing jets are frequently seen in astronomical objects, one of the best studied being SS433. Its extended nebula exhibits a characteristic “S” profile that has been attributed to a precessing jet (Hjellming & Johnston 1981) with great success. Code derived from the work of R. E. Spencer (priv. comm.) was adapted for CH Cygni by removing the relativistic behaviour of the jets. This code gives the on-the-sky positions of discrete knots in the jet at a given time, as determined by a set of parameters. These patterns were compared to the distribution of the 40 brightest CLEAN components in each map at a given frequency and the deviation minimised through use of the Downhill Simplex Method (Nelder & Mead 1965).

The process was carried out using the set of 5 GHz maps taken by the VLA in the highest resolution “A” configuration, as these provided the most extensive coverage of the system over time.

4.1 Simple ballistic model

The simplest model of radio jet precession is one in which material is ejected continuously, at a constant velocity, from the poles of a precessing object. The locus described by the

Table 3. Fitted parameters for the simple ballistic model of jet ejection and precession.

Parameter	Value
P	6519 ± 153 days
T_0	$\text{JD}2444038 \pm 128$
θ_{mid}	$140^\circ \pm 1^\circ$
θ_0	$35^\circ \pm 1^\circ$
v_0	$1263 \pm 18 \text{ km s}^{-1}$
i	$88^\circ \pm 1^\circ$

points along the resulting curved path at a time t is described (see Figure 2) in parametric form by

$$x = v_0(t - \tau) \cos\theta_0 \quad (2)$$

$$y = v_0(t - \tau) \sin\theta_0 \sin(\phi) \quad (3)$$

$$z = v_0(t - \tau) \sin\theta_0 \cos(\phi) \quad (4)$$

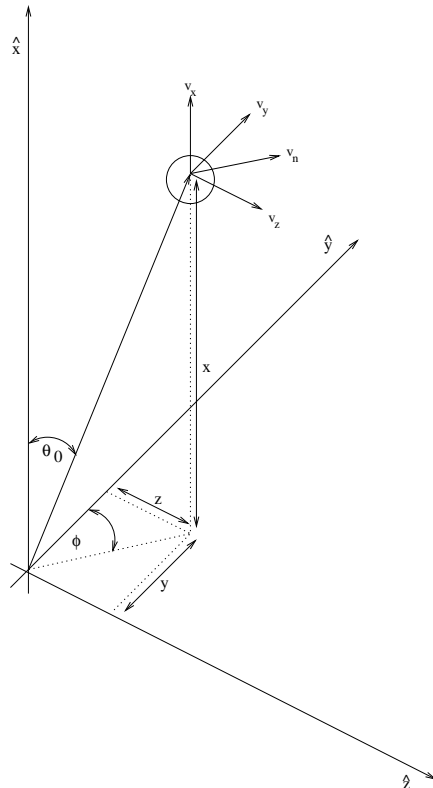
where x , y and z are the coordinates of a given knot of material, ejected from the central source (at the origin) at a time τ with velocity v_0 . The opening angle of the precession cone is θ_0 , measured from the x axis, and the azimuthal angle of the jet (relative to the y axis) is $\Phi = \Omega\tau$ where Ω is the precession rate.

Such a model has been used to fit curves to the high-velocity jets of the microquasar SS433 by Spencer (1984). For this model, the parameters were: P , the precession period of the jet ($= \frac{2\pi}{\Omega}$); τ_0 , a fixed time corresponding to a point when the precession angle of the jets was along the line of sight (the y axis in Figure 2); θ_{mid} the position angle (on the sky) of the axis of precession; θ_0 , the opening angle of precession cone; v_0 , the velocity of the material ejected in the jet and i , the inclination angle of the precession axis to the line of sight.

The size of the initial simplex was set up so that it had parameters centred around $P = 5294$ days (Hinkle et al. 1993), $T_0 = \text{JD}2446275$ (Mikolajewski et al. 1990a), $\theta_{\text{mid}} = 140^\circ$, $\theta_0 = 30^\circ$ (Section 3), $V = 1230 \text{ km s}^{-1}$ (Paper I) and $i = 90^\circ$. The process was allowed to run until the standard errors of the evaluated fits became smaller than 0.01. The “best-fit” parameters from this run were then fed in as the starting values for a second run. This process was repeated so that four runs were carried out. The final set of parameters is shown in Table 3. Results very similar to this were found if the starting period was set to 8373 days, as found in Section 3. The resulting ephemerides, resulting from material being ejected in discrete bullets every 50 days and following the model described above, are shown in Figures 3 and 4.

The model fits reasonably well to the geometry seen in the maps, especially in those resulting from observations closely following the emergence of the radio jet in 1986. In these images (JD2446509 and JD2446576) the jets are two-sided and well extended, making fitting more robust.

In later epochs, when the jet is more one-sided, the curves still fit the morphology seen in the radio maps well. The fact that such a fit is achieved so long after the initial outburst (and following at least two other outbursts) demonstrates that the behaviour of the bipolar jets is not far from a simple ballistic model of the kind applied successfully to SS433 and other sources.

**Figure 2.** Coordinate system used to describe a simple precessing jet. The hot component is at the origin, and the jet is represented by discrete packets of material with coordinates (x, y, z) .

4.2 Disrupted jet model

The greatest deviations of the simple model from the observations are seen in the 1991 map (which has a low peak brightness and high background noise level) and in the motion of the NW component in the 1987 and 1988 maps. If the component is the same object in all of the maps, then it is moving in a fashion entirely different to a simple, ballistic, bullet of material. By inspection, it appears to be decelerating, perhaps due to interaction with dense material.

The synchrotron theory put forward in Paper I required ejecta to be impacting upon previously ejected stellar wind material, in order to cause shocks and local condensations in the magnetic field. This might be expected to cause some degree of deceleration and disruption.

Direct evidence of deceleration is provided by optical spectroscopy (Skopal et al. 2001), which detects the velocity of material within a few hundred R_\odot of the central stars. Terminal velocities of up to 2500 km s^{-1} are seen. Radio maps, which observe the motion of material much further out (from a few AU up to 100s of AU), never detect on-the-sky velocities of more than 1500 km s^{-1} , assuming a distance to CH Cygni of 268 pc (Viotti et al. 1998). This is evidence of a large degree of deceleration between these two scales.

The actual offsets of the apparently-slowed component from the central radio peak at the different observing epochs are shown in Table 4.

A component moving ballistically, as described in Section 4.1, would exhibit a constant position angle (θ_{PA}) and

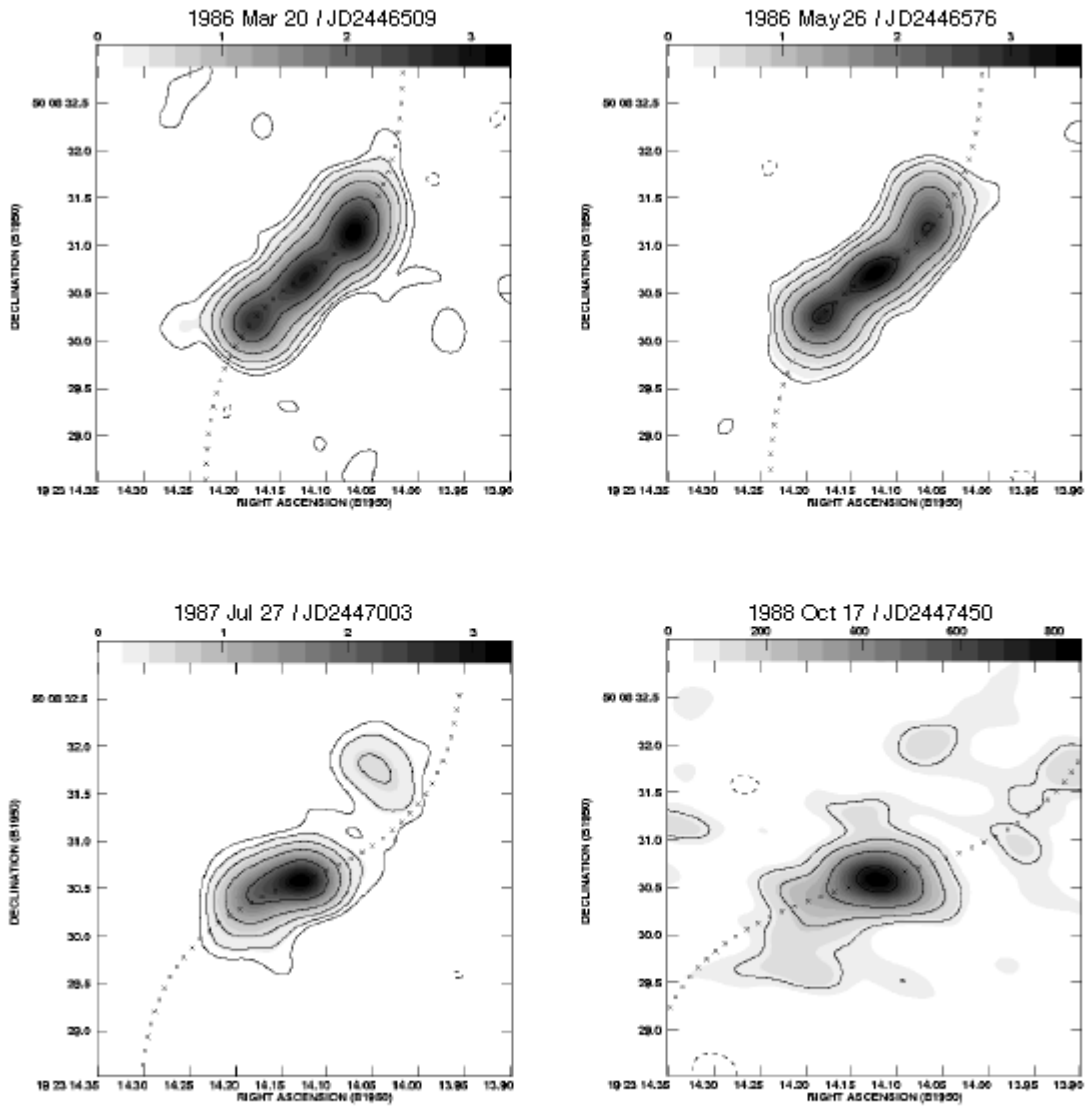


Figure 3. Fitted ballistic material ejection model overlaid upon VLA 5GHz radio maps (1986-1988).

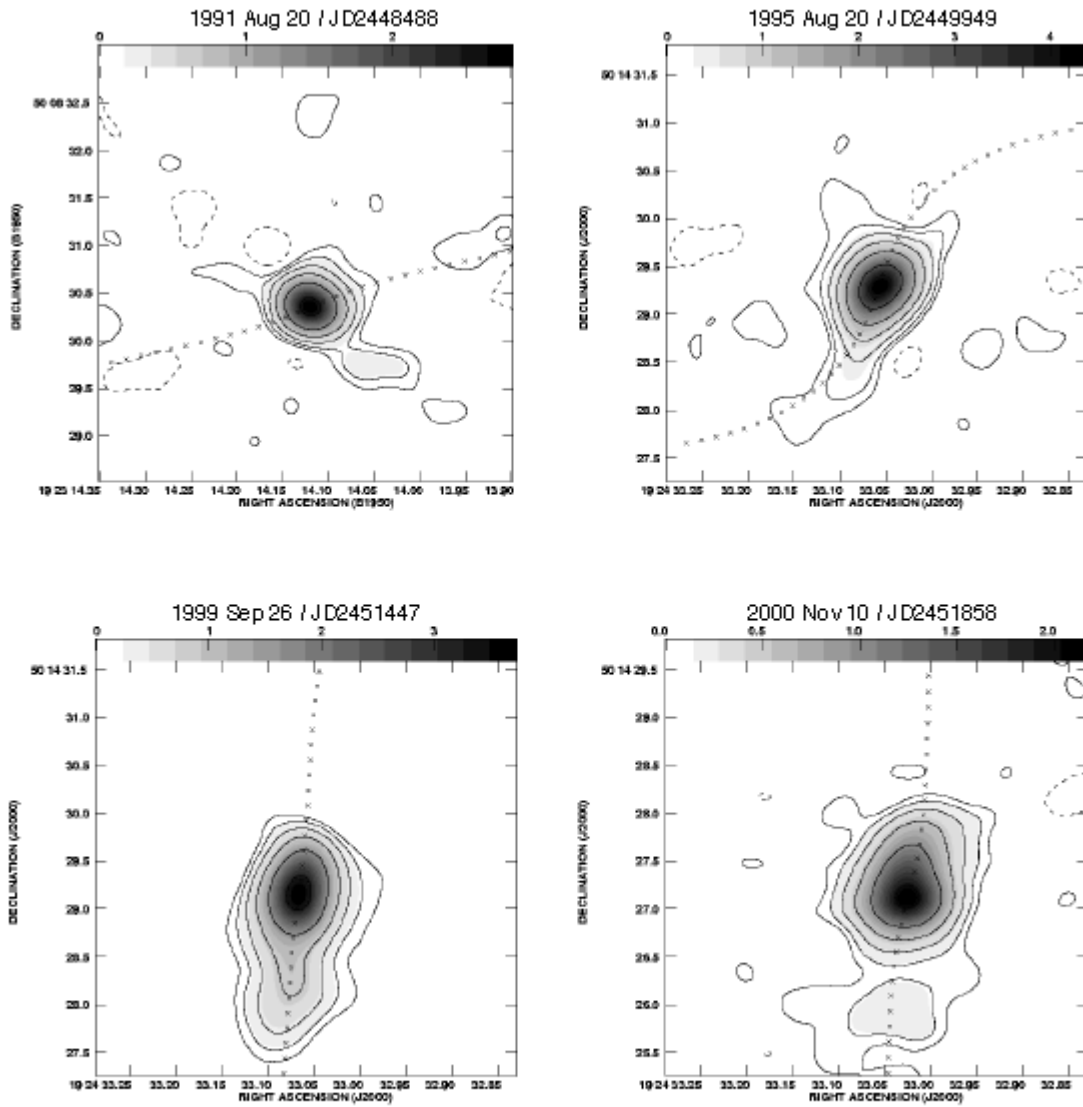


Figure 4. Fitted ballistic material ejection model overlaid upon VLA 5GHz radio maps (1991-2000).

Table 4. Offsets of the anomalous northwestern component of the radio jet of CH Cygni.

Date	Band	Offset (mas)		θ_{PA} ($^\circ$)	R (mas)
		RA	Dec		
2446509	U	671 ± 15	904 ± 13	323.4 ± 1.0	1130 ± 10
2446576	U	546 ± 47	902 ± 20	328.8 ± 2.8	1050 ± 30
2447003	C	773 ± 75	1195 ± 29	327.1 ± 1.8	1420 ± 30
2447450	C	532 ± 75	1430 ± 49	339.6 ± 3.2	1530 ± 50

a radial distance from the core (R) that increased linearly with time. If there is simple deceleration, θ_{PA} would remain constant while R changed according to an environment-dependent model.

Compared with the $\sim 1230 \text{ km s}^{-1}$ velocity seen in the main portion of the jets, the north western emission is almost stationary on the sky. It is possible that the material has indeed almost stopped moving, perhaps due to interactions with the surrounding environment. The jet may have become entirely disrupted through shock-interactions and so would no longer obey the simple ballistic model.

For a jet that has a time-variable ejection direction, such as a precessing bipolar jet, shocks will form between the jet material and the surrounding medium not only in the main direction of jet propagation but also as a result of the transverse interactions between the two regions (Dyson 1987).

The transverse velocity of the jet becomes an important factor at large distances from the point of ejection.

A collimated outflow will only survive until the transverse shock has crossed the diameter of the jet. To simplify things, the approximation of Raga et al. (1993) is used so that

$$t_d \approx \sqrt{\frac{r_j}{\beta v_0 \Omega \sin \theta_0}}. \quad (5)$$

Most of these values can be estimated from work already carried out. The jet radius, r_j , can be estimated by measuring the size of the anomalous region in the 1986 VLA U band map. The region was found to be approximately circular with a mean diameter of 0.18 arcsec. Assuming a distance of 268 pc this corresponds to a linear size of 6.9×10^{12} m. The initial jet ejection velocity was found in Paper I to be $1.23 \times 10^6 \text{ m s}^{-1}$ which is in agreement with that found by fitting to the purely ballistic ejection model. The rate of precession can be found from the fitted period of 6519 days to be $\Omega = 1.1 \times 10^{-8} \text{ rad s}^{-1}$. The opening angle, θ_0 was estimated previously to be $35^\circ \pm 1^\circ$.

The main unknown is the relative density parameter, β . Following Raga et al. (1993), β is assumed to be constant, so that the ambient medium is entirely homogeneous. This may not be the case, as a constant spherical outflow from a star is expected to produce an ambient density that varies as $\rho_e \propto r^{-2}$, and the presence of a jet would be expected to cause disruptions in the local region. However, without more knowledge of this region, a homogeneous medium is assumed for simplicity. Raga & Noriega-Crespo (1993) derived a ratio of $\rho_e/\rho_j \approx 0.05$ from line ratios in the Herbig-Haro object HH 111 V. If this applies to CH Cygni, then β is approximately equal to 0.2.

Applying these parameters to Equation 5 gives a value

for the time taken for the disruptive shock to cross the jet as $t_d \approx 7 \times 10^7$ s. The distance the material has covered in this time (along the x axis in Figure 2) will be, for the parameters discussed above, $x_d = 311$ AU. The actual distance of the observed anomalies in the radio jet in 1986–1988 is indeed around 300 AU.

To determine whether this disruption is occurring, direct imaging of the shocked region is necessary. This has been done in the case of the Herbig-Haro objects HH46/47 (Reipurth & Heathcote 1991) and HH34 (Reipurth & Heathcote 1992). $H\alpha$ maps were subtracted from [S II] maps (at wavelengths 6717Å and 6731Å) to produce images in which the leading bow shock and trailing jet shock could be seen separately. The ratio of the intensity of emission in the $H\alpha$ and [S II] was then used to derive the relative densities in the jet material and surrounding medium (Raga & Noriega-Crespo 1993). Unfortunately, whilst $H\alpha$ emission maps of CH Cygni exist (Paper II), no maps in [S II] are available.

4.3 Models with reflective symmetry

If the geometry of the jets is a result of them being gravitationally attracted to the outer giant, they would be expected to exhibit a morphology in which the position angle of the material is a function of distance from the ejection source, and in which there is reflective symmetry about the central core (Zaninetti & van Horn 1988). Such a model was applied successfully to 3C449 by Lupton & Gott (1982). Such a pattern does not fit the observed extensions in the CH Cygni system, implying that the precession is due to effects within the collimating mechanism, rather than post-ejection gravitational influences.

4.4 Ballistic model with time-dependent ejection velocity

CH Cygni is observed to undergo irregular outbursts with associated variable mass outflow rates. Such a state of affairs renders invalid the assumption that what is being observed is a simple, continuous jet with constant ejection velocity. A jet that results from truly irregular outflows is difficult to model analytically using the methods described within this work.

Recent work, as described in Paper II, has discovered what may be two types of mass outflow from the system. One is optically thin, at a velocity measured spectroscopically to be 1200 km s^{-1} and the other is optically thick and highly irregular. There is evidence that the increase in mass-transfer from the cool component to the compact component that occurs near to times of periastron leads to higher luminosity of the compact component and, as a consequence, greater radiatively driven mass outflow.

Assuming a distance of 268 pc (Viotti et al. 1998), the movement between 1986 and 1988 shown in Table 4 represents an on-the-sky velocity of only $\sim 200 \text{ km s}^{-1}$. Extrapolating this motion backwards gives the time of ejection of this material, assuming ballistic motion, as around December 1978. This time is near the beginning of the large outburst that lasted between 1977 and 1984. Minor outflows have been observed spectrally during the outburst (Hack et al. 1988; Anderson et al. 1980) at velocities of a few hun-

dred km s^{-1} . These may coincide with the ejection of this anomalous packet of material.

Recent HST observations (from October 1999) made by Corradi et al. (2001) show the existence of loops of material in the [OII] nebula at a distance of ~ 1.5 and ~ 5 arcsec. Echelle spectroscopy of these loops places their kinematical axis at around 100 km s^{-1} . Allowing for projection effects (i.e. assuming they are tilted at 37° to the plane of the sky) their kinematical ages are approximately 15.2 years for the inner loop and 51 years for the outer one, giving the times of ejection of the loops as August 1984 and February 1949 respectively. The 1984 event fits in well with the emergence of the radio jets first observed by Taylor et al. (1986) and the model proposed in this section, but no records of a 1949 outburst could be found (Mikolajewski et al. 1990a).

5 POSSIBLE CAUSES OF PRECESSION

Precession of bipolar jets is a common phenomenon in astrophysics (Fukue & Yokoo 1986). The precession is usually attributed to motion of the collimating mechanism of the jets.

A simple collimating structure is a circumstellar torus or disk, such as that postulated by Fukue (1983). Flickering in the optical brightness of CH Cygni has been observed on several occasions (Wallerstein 1968; Mikolajewski et al. 1990b) and has been explained by the orbital motion of a bright point on a disk surrounding the compact component.

There are several mechanisms by which such a disk could be induced to precess, and four of these scenarios are examined here. Only one of these is able to cause precession at the rate that is observed, given suitable estimates for the appropriate parameters.

5.1 Precession of a tilted accretion disk

The gravitational influence of the nearby cool component, or perhaps the possible third star in the system, could force precession in this disk, and hence the jets. Following the work of Merritt & Petterson (1980), the angular speed of a torus or disk, with radius r , undergoing forced precession as a result of the influence of a companion is

$$\Omega = -\frac{3}{4} \sqrt{\frac{G}{m_h}} \frac{m_h m_c}{m_h + m_c} \frac{r^{\frac{3}{2}}}{a^3} \cos \alpha$$

where m_h is the mass of the hot component, m_c is the mass of the cool component, a is their separation and α is the angle between the equatorial plane of the torus and the orbital plane of the stars. Estimates for the parameters, from the work of Skopal (1997), are $m_h = 0.2M_\odot$, $m_c = 0.93M_\odot$ and $a = 1.5 \text{ AU}$. This relation assumes that the disk is centred on the hot component, and the companion star causing the forced precession is the cool giant on the 756 day orbit. It would also be sensible to assume that $\alpha < 45^\circ$ (Mikolajewski et al. 1990b) and $0 < r < a$. To obtain a precession period of 8373 days requires a disk radius of around 0.7 AU. This is a very large accretion disk, and it would be hard to imagine how such a disk could form purely via wind accretion mechanisms, making this scenario unlikely.

If instead it is assumed that CH Cygni is a binary system on a 5294 day orbit, with $a = 7.9 \text{ AU}$ the disk radius is found to be around 21 AU, around twice the size of the proposed semimajor axis of the outer giant's orbit.

5.2 Slaved disk

An attempt to explain the observed 164 day period precession of the bipolar jets in SS433 was made by van den Heuvel et al. (1980), by assuming that the compact component was surrounded by an accretion disk that precessed at a rate governed by the apsidal motion of the parent star.

Using Equations 12, 13 and 16 of that paper, taking reasonable stellar and orbital parameters of CH Cygni from Skopal (1997) and assuming that the coefficient of apsidal motion is 0.005 (Schwarzschild 1958) suggests that the precession period of a slaved disk would be around 12000 years. This result is a strong function of the radius of the cool component, so an increase in this star's size by a factor of 4 would reduce this precession period to about 15 years.

To evaluate the possibility of such a model, precise eclipse timings need to be made in the future.

5.3 Irradiated disk

An accretion disk that is irradiated by a central source can become warped as a result of a torque that arises due to radiation that is re-emitted from the disk (Livio & Pringle 1997).

Such a warped disk might be expected to precess. In contrast to the gravitationally induced precession mentioned above, this is "self precession", in that no companion star is required. Following the work of Livio & Pringle (1996), the period of this precession is of the same order as the time it takes for the warping to develop in the disk. Using sensible parameters for the mass of a possible accretion disk (around $10^{-7} M_\odot$), this timescale is of the order of ~ 2000 years, making this an unsuitable model for precession.

5.4 Magnetic precession

The inner region of an accretion disk surrounding a magnetic star, such as a white dwarf (Mikolajewski et al. 1990b), is subject to a twisting torque and a warping torque. These arise as a result of the interaction between the surface current of the disk and the horizontal magnetic field that is a feature of the dipole field of the star (Lai 1999).

The warping torque arises through the twisting of the field that threads the disk vertically. The precessing torque is a result of the azimuthal screening current that occurs if the disk is diamagnetic. In this case, the vertical field lines cannot penetrate the disk. An azimuthal current is induced in the disk. The radial component of the central star's magnetic field interacts with this current to set up a vertical force acting on the disk. This force is uneven across the disk, so a net torque results. This torque acts to cause the disk (and hence the collimation mechanism of the jets) to precess about the magnetic axis of the star.

Lai (1999) gives the angular precession rate of such a disk in Equation 2.35 of that paper. Presently, most of the

required quantities are unknown, so only an order of magnitude estimate is possible. The magnetic moment of the white dwarf was estimated to be $2 \times 10^{28} \text{ T m}^3$ using the method of Postnov (1985), and the surface density of the disk was assumed to be of the order 10 kg m^{-2} (Lin et al. 1988). The angle between the disk axis and stellar rotation axis was taken to be equal to the opening angle of the precession cone, 35° , found previously. The magnetic axis of the system was assumed to lie along the disk axis.

The magnetically induced precession period is then directly related to the radial distance, r , of the warped torus from the white dwarf. Since this varies as r^7 , small changes in r greatly affect the period. A warped torus at around $2 R_\odot$ from the star will precess with a period of around 6000 days.

A magnetic collimation and ejection mechanism for the jets gives a possible explanation for their one-sidedness (Chagelishvili et al. 1996). Jets powered by a central magnetic rotator (Mikolajewski et al. 1990b) can become inherently asymmetric, if the solution to the magnetohydrodynamic equations for each hemisphere of the star are asymmetric. Such conditions arise when there is no change in the relative sign of the poloidal and toroidal fields across the equator of the star. The different magnetic states above and below the equator can then easily lead to a condition in which only one supports the collimation and ejection of material via a jet (Wang et al. 1992).

6 CONCLUSION

It is certain that the bipolar jets of CH Cygni exhibit precession, with a period controlled by the motion of the mechanism responsible for the collimation of the outflow. In addition, the variability of the mass-loss rate from the cool component causes the material to be ejected at a rate that is highly variable (between ~ 500 and 2000 km s^{-1}), leading to complications in predicting the outflow geometry. The activity of the bipolar ejection seems to be tied to the state of the hot-component, with fast jets seen at or soon after times of optical outburst. This activity then decreases during times of quiescence.

Although the precession period found here is similar to the orbital period of the outer giant in the system, the current time resolution of the observations does not rule out shorter periods. A precession that resulted from the motion of the inner, symbiotic, pair and had a similar period to its 756 day orbit would need observations to be taken at least every year for it to be detected.

The simple ballistic model fits the geometry of the nebula extremely well. Knots seen in the larger-scale radio maps (the VLA in C, X and U band) that do not fit the simple ballistic model can be explained as regions of jet disruption caused by sideways motion of the ejected material brought about as a result of the precession. The predicted distance at which this disruption would occur is in close agreement with the observations, although it relies upon several assumptions about the nature of the ambient material. Confirmation of this model would require simultaneous optical images in both $H\alpha$ and $[S II]$.

An alternative explanation is that the anomalous material was ejected at a much slower velocity and at an earlier time than the majority of the gas in the bipolar nebula.

This would indicate the presence of a minor ejection event prior to the main ejection of the jets first seen by Taylor et al. (1986). The variable ejection velocity model discussed here and the Echelle spectroscopy of Corradi et al. (2001) suggest the emission of material with a velocity of no more than a few 100 km^{-1} just before the main ejection of the high-speed material.

The cause of the precession is unknown but, given realistic estimates for the masses and separation of the stellar components, warping of the collimating accretion disk by a magnetic white dwarf is the only mechanism that can give precession periods similar to those found by model fitting. The other possible causes give periods that are several orders of magnitude too large. The magnetic explanation also allows for the one-sided nature of the emission seen in all VLA radio maps following the initial outburst in 1984.

ACKNOWLEDGMENTS

MC is supported by a grant from the Particle Physics and Astronomy Research Council (PPARC). The contribution of AS was supported by a grant of the Slovak Academy of Science, number 2/1157/01. The VLA is operated by the National Science Foundation operated under cooperative agreement with Associated Universities, Inc. MERLIN is a national facility operated by the University of Manchester on behalf of PPARC. Ultraviolet spectral data are based on INES data from the IUE satellite, operated by ESA.

REFERENCES

- Anderson C.M., Oliverson N.A., Nordstieck K.H., 1980, *ApJ*, 242, 188
- Biretta J., et al., 2001, *WFPC2 Instrument Handbook, Version 5.0*. STScI
- Chagelishvili G.D., Bodo G., Trussoni E., 1996, *A&A*, 306, 329
- Corradi R.L.M., Munari U., Livio M., Mampaso A., Gonçalves D.R., Schwarz H.E., 2001, *ApJ*, In press
- Crocker M.M., Davis R.J., Eyres S.P.S., Bode M.F., Taylor A.R., Skopal A., Kenny H.T., 2001, *MNRAS*, 326, 781
- Dyson J.E., 1987, In Appenzeller I., Jordan C., eds., *IAU Symp. 122: Circumstellar Matter*, vol. 122, pp. 159–172
- Eyres S.P., Kenny H.T., Cohen R.J., Lloyd H.M., Dougherty S.M., Davis R.J., Bode M.F., 1995, *MNRAS*, 274, 317
- Eyres S.P.S., Bode M.F., Skopal A., Crocker M.M., Davis R.J., Taylor A.R., 2001a, *MNRAS*, Submitted
- Eyres S.P.S., Bode M.F., Taylor A.R., Crocker M.M., Davis R.J., 2001b, *ApJ*, 551, 512
- Fukue J., 1983, *PASJ*, 35, 539
- Fukue J., Yokoo T., 1986, *Nature*, 321, 841
- Greisen E., 1999, *The AIPS cookbook*, NRAO, Charlottesville, Virginia, USA, chap. 5
- Hack M., Engin S., Rusconi L., Sedmak G., Yilmaz N., Boehm C., 1988, *A&AS*, 72, 391
- Hack W.J., Paresce F., 1993, *PASP*, 105, 1273
- Hinkle K.H., Fekel F.C., Johnson D.S., Scharlach W.W.G., 1993, *AJ*, 105, 1074
- Hjellming R.M., Johnston K.J., 1981, *ApJ*, 246, L141

- Högbom J.A., 1974, *A&AS*, 15, 417
- Iijima T., 1996, *Astro. Lett. and Communications*, 34, 327
- Kenny H.T., et al., 1996, In Taylor A.R., Paredes J.M., eds., *Radio emission from the stars and the sun*, vol. 93, p. 197
- Lai D., 1999, *ApJ*, 524, 1030
- Leedjävrv L., Mikolajewski M., 1996, *A&A*, 300, 189
- Lin D.N.C., Williams R.E., Stover R.J., 1988, *ApJ*, 327, 234
- Livio M., Pringle J.E., 1996, *ApJL*, 465, L55
- Livio M., Pringle J.E., 1997, *ApJ*, 486, 835
- Lupton R.H., Gott J.R., 1982, *ApJ*, 255, 408
- Merril P.W., 1941, *PAAS*, 10, 168
- Merritt D., Petterson J.A., 1980, *ApJ*, 236, 255
- Mikolajewski M., Tomov T., 1986, *MNRAS*, 219P, 13
- Mikolajewski M., Mikolajewska J., Tomov T., 1987, *AP&SS*, 131, 733
- Mikolajewski M., Mikolajewska J., Khudyakova T.N., 1990a, *A&A*, 235, 219
- Mikolajewski M., Mikolajewska J., Tomov T., Kulesza B., Szczerba R., 1990b, *Acta Astronomica*, 40, 129
- Nelder J.A., Mead R., 1965, *The Computer Journal*, 7, 308
- Postnov K.A., 1985, *Soviet Astronomy*, 29, 650
- Raga A.C., Noriega-Crespo A., 1993, *Rev. Mexicana Astron. Astrof.*, 25, 149
- Raga A.C., Canto J., Biro S., 1993, *MNRAS*, 260, 163
- Reipurth B., Heathcote S., 1991, *A&A*, 246, 511
- Reipurth B., Heathcote S., 1992, *A&A*, 257, 693
- Richards A.M.S., Bode M.F., Eyres S.P.S., Kenny H.T., Davis R.J., Watson S.K., 1999, *MNRAS*, 305, 380
- Schwarzschild M., 1958, *Structure and evolution of the stars*. Princetown University Press
- Seaquist E.R., Taylor A.R., Button S., 1984, *ApJ*, 284, 202
- Skopal A., 1997, In Mikolajewska J., ed., *Physical processes in symbiotic binaries*, Copernicus Foundation for Polish Astronomy, pp. 99–104
- Skopal A., Bode M.F., Lloyd H.M., Tamura S., 1996, *A&A*, 308, L9
- Skopal A., Bode M.F., Crocker M.M., Drechsel H., Eyres S.P.S., Kenny H.T., Komžík R., 2001, *MNRAS*, In prep
- Skopal A., et al., 1996, *MNRAS*, 282, 327
- Spencer R.E., 1984, *MNRAS*, 209, 869
- Taylor A.R., Seaquist E.R., Mattei J.A., 1986, *Nature*, 319, 38
- van den Heuvel E.P.J., Ostriker J.P., Petterson J.A., 1980, *A&A*, 81, L7
- Viotti R., Badiali M., Cardini D., Emanuele A., Iijima T., 1998, 1997 *Hipparcos*, ESA, p. 405
- Wallerstein G., 1968, *The Observatory*, 88, 111
- Wang J.C.L., Sulkanen M.E., Lovelace R.V.E., 1992, *ApJ*, 390, 46
- Zaninetti L., van Horn H.M., 1988, *A&A*, 189, 45